

Emulsifying Properties of Bovine Serum Albumin–Galactomannan Conjugates

HYUN JUNG KIM,[†] SEUNG JUN CHOI,[†] WEON-SUN SHIN,[‡] AND TAE WHA MOON^{*,†}

Department of Food Science and Technology, School of Agricultural Biotechnology and Center for Agricultural Biomaterials, Seoul National University, Suwon 441-744, Korea, and Korea Food Research Institute, Sunnam 463-420, Korea

Bovine serum albumin (BSA)–galactomannan conjugates were prepared through the Maillard reaction. To 1 mol of BSA was bound 2.5–7 mol of galactomannan. Conjugates could be grouped into two fractions, on the basis of the weight-average molar mass measured with a multiangle laser light-scattering detector, the main one with 220 000–250 000 Da and the other one with a very small amount of aggregates over 1 000 000 Da. Spectroscopic analysis suggested that the surface of the conjugate was covered with galactomannan and the conformation of the hydrophobic interior and the secondary structure were not significantly changed. The emulsifying activity index of the conjugates increased greatly as compared with that of BSA alone. All conjugates showed better stability than BSA, presumably due to the physical protection introduced by the viscoelastic galactomannan layer. The average particle sizes of the emulsions were similar. The interfacial properties of the BSA–galactomannan conjugates were improved, possibly due to the reduced hydrophobic interaction between the droplets and the viscoelastic interfacial properties of galactomannan.

KEYWORDS: Bovine serum albumin–galactomannan conjugates; multiangle laser light scattering; fluorescence; circular dichroism; emulsion properties

INTRODUCTION

Proteins contribute significantly to the textural and sensory attributes of various foods (1, 2). Important functional properties of food proteins include solubility, viscosity, oil and water binding, gelation, foaming, and emulsifying properties. However, these diverse properties are sensitive to environmental factors such as solvent nature, pH, temperature, and ionic strength (3, 4).

Another important type of structure-forming macromolecules is the polysaccharides, which express distinct functional properties in food systems (5). They have been used as thickening, gelling, and suspending agents and as stabilizers in foams and emulsions. However, the low surface activity of polysaccharides limits their utilization as foaming or emulsifying agents alone.

Thus, many researchers have tried to improve proteins' stability and functionality in foods by mixing proteins and polysaccharides (6, 7). However, the mere mixing of these macromolecules creates mostly nonspecific and noncovalent interactions, which are sensitive to environmental conditions. Accordingly, aggregation or phase separation can occur due to the depletion flocculation or thermodynamic incompatibility of the two macromolecular components (8, 9). Therefore, as a compensation, covalent bonding, which maintains structural

integrity under various conditions, has been introduced (10–14). However, focus had been placed mainly on improving the functionality; hence, the structural rationale of the conjugate and improved functionality is not fully understood yet.

Bovine serum albumin (BSA), which is stabilized by 17 disulfide bonds and endowed with a compact and rigid structure (15), has been studied mainly because it is a major component of bovine plasma, one of the massive wastes from slaughterhouses. Various biological, physicochemical, and structural properties of serum albumins have been extensively investigated, including the domain structure, which makes BSA a desirable model protein for the food systems (16, 17). In addition, the physicochemical properties of BSA could be modified for diverse functional applications.

Galactomannan is composed of (1→4)-linked β -D-mannopyranosyl residues, substituted at O-6 by a single α -D-galactopyranosyl unit, and is obtained from seed gums such as locust bean gum and guar gum (18). Although the degree of galactose substitution and resultant physicochemical properties vary from one botanical source to another, galactomannan has relatively high water solubility, forms highly viscous solutions, and has been used as a thickener, binder, and stabilizing agent in foods (19, 20). It is not expensive and can be easily obtained commercially, which makes it a suitable raw material for the preparation of protein–polysaccharide conjugates.

The main objective of this study was to obtain information on the structural characteristics and emulsifying properties of

* To whom correspondence should be addressed (telephone 82-31-290-2581; fax 82-31-293-4789; E-mail twmoon@snu.ac.kr).

[†] Seoul National University.

[‡] Korea Food Research Institute.

the BSA–galactomannan conjugate formed through the Maillard reaction. On the basis of this information, improvements in the emulsion properties of conjugates could be more clearly understood. For elucidation of the influence of bound polysaccharide and its amount on protein conformation, conjugates in varying ratios were examined using colorimetric and spectroscopic methods. The molecular weight and radius of gyration were investigated using a multiangle laser light-scattering detector. Various emulsion properties of the conjugates were also investigated.

MATERIALS AND METHODS

Materials. BSA (fraction V, A-6793) was purchased from Sigma Chemical Co. (St. Louis, MO). Galactomannan (mannase hydrolysate of guar gum, average molecular weight 22 000) was obtained from Taiyo Chemicals Co. (Nagoya, Japan) and was used after dialysis against distilled water using a molecular weight cutoff 12 000–14 000 dialysis membrane (Spectrum Medical Industries, Inc., Houston, TX). All other chemicals were of analytical reagent grade.

Preparation and Binding Pattern of BSA–Galactomannan Conjugates. BSA–galactomannan conjugates were prepared through the Maillard reaction. Each BSA–galactomannan mixture, at molar ratios of 1:3, 1:6, 1:9, 1:12, and 1:15, was dissolved in deionized distilled water to the final concentration of 1% (w/v) and freeze-dried. The mixtures were stored at 60 °C and 79% relative humidity in a desiccator containing a saturated KBr solution in the bottom for 3 days (21). For purification, products in various ratios were dissolved in deionized distilled water at 0.25% (w/v) concentration and filtered through a 0.45- μ m pore-sized polyethersulfone membrane filter (Whatman International Ltd., Maidstone, UK) to remove undissolved aggregate. Ultrafiltration was then conducted with a YM-100 membrane (Amicon Inc., Beverly, MA) to retain the product until half of the initial volume remained, followed by adding deionized distilled water to the original volume. This procedure was repeated three times, and the resulting solution was concentrated 5-fold using a YM-100 ultrafiltration membrane. The retentates containing soluble product were freeze-dried and stored at 4 °C. Freeze-dried soluble products are referred to as BSA–galactomannan conjugates hereafter. Final yields of the conjugates were 67.3 ± 0.7 , 57.6 ± 2.2 , 43.1 ± 2.5 , 41.9 ± 2.2 , and $31.6 \pm 0.4\%$ for 1:3, 1:6, 1:9, 1:12, and 1:15 reactants, respectively.

Sodium dodecyl sulfate–polyacrylamide gel electrophoresis (SDS–PAGE) (22) was carried out to confirm the formation of conjugate with an 8% separating gel and a 5% stacking gel. Samples dissolved in 0.01 M phosphate buffer (pH 7.4) were heated at 100 °C for 5 min in 60 mM Tris–HCl buffer (pH 6.8) with 2% SDS and 14.4 mM mercaptoethanol. Sample solutions of the conjugates with equal amounts of protein (10 μ g) were loaded into each well. Development was done at a constant 20 mA for 4 h with 0.1% Tris–glycine electrophoresis buffer (pH 8.3). The gel was stained for protein detection with Coomassie Brilliant Blue R (23) and destained in a solution containing 10% methanol and 10% acetic acid. Glycoprotein staining was conducted with fuchsin after fixation, and destaining was conducted with 0.5% sodium metabisulfite solution (24, 25). The binding ratio of galactomannan to BSA was estimated using the colorimetric method. The BSA content was calculated on the basis of the absorbance at 595 nm using a Bio-Rad Protein Assay Kit (Bio-Rad Laboratories, Hercules, CA) following Bradford's method (26). The galactomannan content was measured using the phenol–sulfuric acid method at 490 nm (27).

Structural Characteristics of BSA–Galactomannan Conjugates. The weight-average molar mass (M_w) and the root-mean-square radius, also called the radius of gyration (R_g), relating to the distribution of mass within the molecule, were determined using high-performance size-exclusion chromatography. The mobile phase was 0.067 M phosphate buffer (pH 7.0) containing 0.1 M NaCl, which had been filtered consecutively through 0.2- and 0.1- μ m cellulose nitrate membrane filters (Whatman International Ltd.). The BSA–galactomannan conjugate was dissolved in the buffer (10 mg/mL) and filtered through a 0.45- μ m polysulfone filter (Millipore Corp., Bedford, MA). It was passed through a 0.1- μ m pore-size in-line filter, and a 20- μ L

aliquot was subjected to a high-performance size-exclusion chromatography system, which consisted of a Shodex OHPak guard column, a TSK Gel 4000 PWXL column (Tosoh Co., Tokyo, Japan), and a Shodex OHPak SB-805 column (Showa Denko, Tokyo, Japan), at a flow rate of 0.3 mL/min. A multiangle laser light-scattering detector (Dawn DSP-F, Wyatt Technology, Santa Barbara, CA) with a helium–neon laser source ($\lambda = 632.8$ nm) and a refractive index (RI) detector (Opti-Lab, Wyatt Technology) were used. Output voltage values of the refractive index detector and multiangle laser light-scattering detector at 18 angles were collected and applied to a Debye plot for the calculation of M_w and R_g using Astra 4.70 software (28). The specific refractive index increment (dn/dc) was measured for each sample in the elution buffer described above with the RI detector and used for M_w calculation.

Fluorescence measurement was performed with an F-4500 fluorescence spectrophotometer (Hitachi Ltd., Tokyo, Japan) using a 1-cm-path length quartz cuvette at 25 °C, as described by Kella et al. (29). Conjugate solutions were prepared in 0.01 M phosphate buffer (pH 7.4). Intrinsic fluorescence measurement of 0.05 mg/mL protein solution was carried out with excitation at 279 nm and emission scanning in the range of 300–400 nm. For extrinsic fluorescence measurement, a mixture of 0.1 mg/mL protein and 40 μ M 1-anilino-8-naphthalene-sulfonic acid was excited at 350 nm, and the emissions were scanned in the range of 400–650 nm. Slit widths were 5 and 10 nm for excitation and emission, respectively.

Circular dichroic spectra of BSA and the conjugates in varying ratios were obtained using a Jasco J-715 spectropolarimeter (Jasco Inc., Tokyo, Japan). The spectral bandwidth was 2 nm, and the time constant was 2 s at 25 °C. Data were expressed in molar ellipticity, θ (mdeg). Secondary structure was monitored in the range of 185–250 nm using a 0.1-cm-path length cell at 0.1 mg/mL protein concentration. Ellipticity at 222 nm was examined to calculate the α -helix content using the method of Chen et al. (30).

Measurement of Emulsifying Properties. Emulsifying properties were measured through turbidimetry according to the method of Pearce and Kinsella with a slight modification (31). To prepare emulsions, each sample was dissolved in 0.01 M phosphate buffer (pH 7.4) at 0.1% (w/v) concentration, and *n*-tetradecane was added to an oil volume fraction of 0.2. It was homogenized using an Ultra Turrax T-25 instrument (IKA-Labortechnik, Staufen, Germany) at 21 000 rpm for 1 min at 25 °C. Ten microliters of the emulsion was taken from the bottom of the container and diluted with 1 mL of 0.1 M NaCl solution containing 0.1% SDS. The emulsifying activity was measured as absorbance at 500 nm immediately after the emulsion was made (21). The emulsifying activity index (EAI) was calculated using the following equation (32),

$$\text{EAI} = 2T/(1 - \Phi)C$$

where Φ is the oil volume fraction and C refers to the protein content in milligrams per milliliter. The turbidity, T , is calculated as $2.303A/L$, where A is the observed absorbance and L is the path length of the cuvette. The emulsion stability index (ESI) was determined as follows (33),

$$\text{ESI (min)} = T_0/T'$$

where T_0 refers to turbidity at 0 min after emulsification, T' denotes the change in turbidity between 0 and 30 min, and t is the time interval.

The protein content adsorbed at the oil–water interface was calculated according to the modified depletion method of Dickinson (34). A freshly made emulsion was centrifuged at a low speed of 5090g for 30 min at 25 °C to prevent breakup of emulsion and desorption of loosely bound protein from the interface, and the bottom, denser layer was collected using a syringe. To the cream layer of supernatant was added 0.5 mL of 0.01 M phosphate buffer (pH 7.4), and the same procedure as above was repeated. The collected bottom layer was centrifuged at 9900g for 30 min at 25 °C to remove the remaining cream, and the protein content was measured using Bradford's method. The amount of adsorbed protein was the difference between the initial protein content (mg/mL) in the aqueous phase and the final concentra-

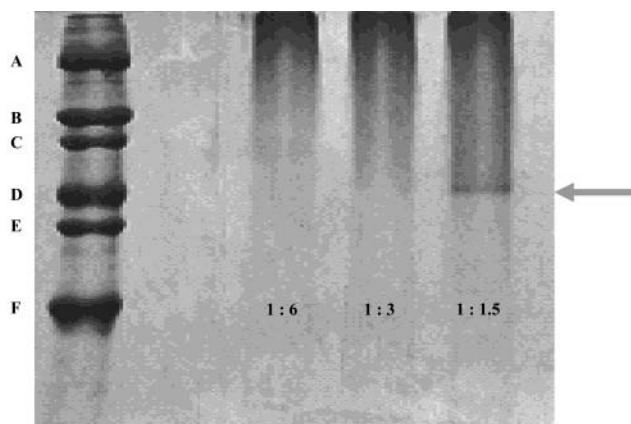


Figure 1. Sodium dodecyl sulfate–polyacrylamide gel electrophoretic pattern of the BSA–galactomannan mixture after 72 h of the Maillard reaction at 60 °C and 79% RH. Molecular weight standards: (A) myosin, 212 kDa; (B) β -galactosidase, 116 kDa; (C) phosphorylase B, 97 kDa; (D) bovine serum albumin, 68 kDa; (E) catalase, 58 kDa; (F) aldolase, 40 kDa. Arrow indicates the BSA remaining after Maillard reaction.

tion determined using Bradford's method after centrifugation. The protein load (mg/m^2) at the oil–water interface was calculated by dividing the amount of adsorbed protein by the interfacial area (IA). The interfacial area was determined on the basis of the absorbance at 500 nm using the equation $IA = 2T$. The turbidity, T , was calculated as described above. The distribution of the emulsion droplet size was measured using Elzone 280PC (Particle Data, Inc., Elmhurst, IL), equipped with a 30- μm -diameter orifice at 25 °C. The counter was calibrated with a 3.14- μm standard latex. A 100- μL sample, taken from the bottom of a container of freshly made emulsion, was diluted 1000-fold with 0.9% NaCl solution. All the data presented are the averages of triplicate measurements made on three separately prepared samples.

RESULTS AND DISCUSSION

Structural Characteristics of Conjugates. SDS–PAGE was conducted to confirm the formation of the BSA–galactomannan conjugate through the Maillard reaction. The initial reaction molar ratios of BSA to galactomannan were 1:1.5, 1:3, 1:6, 1:9, 1:12, and 1:15. In the electropherogram for the 1:1.5 reactant, a band from the remaining BSA, which had not taken part in the reaction, was observed (**Figure 1**). The amount of galactomannan was not sufficient to react with all of the BSA molecules, and excess BSA remained. As no BSA band was observed in the 1:3 reactant, at least 1.5 mol or more of galactomannan was speculated to bind to 1 mol of BSA. Therefore, the 1:1.5 reactant was excluded in the following experiments.

When protein and polysaccharide form a conjugate through a covalent bond, the ϵ -amino residue of the protein and the reducing end of the polysaccharide attach to each other (11, 35, 36). Drags appeared both in the protein and glycoprotein stains for the BSA–galactomannan conjugate, indicating that the complex was polydisperse and had a broad molecular weight distribution (36, 37). In the protein stain, the mixture of BSA and galactomannan showed one band corresponding to the native BSA. However, in the glycoprotein stain, neither galactomannan nor BSA–galactomannan mixtures were detected (**Figure 2**). Thus, connection of BSA and galactomannan by covalent bonds through the Maillard reaction was confirmed.

Assessment of the binding molar ratio of galactomannan to BSA in the product revealed that 2.5 mol of galactomannan was bound to 1 mol of BSA in the 1:3 reaction system, as expected from the electropherogram. With an increase in galactomannan content, up to 7 mol of galactomannan was

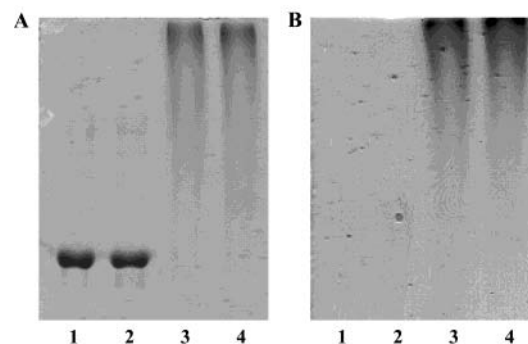


Figure 2. Sodium dodecyl sulfate–polyacrylamide gel electrophoretic patterns of BSA–galactomannan conjugates after isolation. Lane 1, native BSA; lane 2, native BSA–galactomannan mixture; lane 3, 1:6 BSA–galactomannan conjugate; lane 4, 1:12 BSA–galactomannan conjugate. (A) Protein stain; (B) carbohydrate stain.

Table 1. Molar Binding Ratio of BSA–Galactomannan Conjugates at Various Reaction Ratios

molar ratio of BSA to galactomannan reacted	product molar ratio ^a
1:3	1:2.5 \pm 0.2
1:6	1:3.5 \pm 0.5
1:9	1:5.5 \pm 0.4
1:12	1:6.5 \pm 0.6
1:15	1:6.7 \pm 1.0

^a Values are means \pm standard deviation of three independent experiments. Triplicate measurements were performed for each experiment.

bound to 1 mol of BSA (**Table 1**). It appeared that about 3 mol of ϵ -amino residue was present in 1 mol of BSA, which is susceptible to binding with galactomannan. If an excess amount of galactomannan, i.e., more than 9 mol per 1 mol of BSA, is present around BSA, then the binding of galactomannan would increase to above 3 mol per 1 mol of BSA, resulting in an increase of the insoluble fraction estimated from the yield.

M_w and R_g of soluble BSA–galactomannan conjugates were calculated using dn/dc values with a multiangle laser light-scattering system. The dn/dc values measured for BSA, galactomannan, and the 1:3, 1:6, 1:9, 1:12, and 1:15 conjugates were 0.164, 0.135, 0.141, 0.145, 0.134, 0.123, and 0.140, respectively. The quantity R_g gives a rough idea of the volume of solution occupied by the extended molecule. This volume will usually be much greater than that which the molecule would occupy if it were shrunk to a compact sphere. Consequently, when a macromolecule, such as a protein, is denatured, it will expand to effectively enclose a much larger fraction of the total solution volume (38). On the basis of the molecular weight distribution, the BSA–galactomannan conjugates could be divided into two fractions, the main one with 220 000–250 000 and the other with a very small amount of much larger-sized conjugate aggregates (**Table 2**). The smaller fraction constituted more than 97% of all the conjugates formed. The 240 000 fraction (peak 2) in the 1:3 and 1:6 reactants likely consisted of 2 mol of BSA bound with 5 mol of galactomannan. A similar result was also observed in the 1:9 reactant that was fractionated into 250 000 and 4 000 000 parts. This appeared to be a result of the fact that the amount of galactomannan bound in the high-molecular-mass fraction was quite large, and, therefore, galactomannan bound to 1 mol of BSA was not calculated to be greater than the value obtained by colorimetric determination.

In the 1:12 and 1:15 reactants, the 220-kDa fraction was calculated to be comprised of 1 mol of BSA and 7 mol of

Table 2. Weight-Average Molar Mass (M_w) and Radius of Gyration (R_g) of Native BSA–Galactomannan Conjugates As Determined by Second-Order Debye Fitting

sample	M_w (kDa)		R_g (nm)		density (M_w/R_g)
	peak 1	peak 2	peak 1	peak 2	
1:3	1111(16) ^a	245.0(0.3)	38.8(0.1)	15.6(0.6)	13.3
	277.0(0.6) ^b				
1:6	5985(162)	245.0(0.3)	33.1(0.1)	16.7(0.1)	14.0
	256.0(0.4)				
1:9	4001(104)	248.0(0.3)	39.3(0.1)	17.6(0.1)	9.9
	315.0(1.6)				
1:12	1730(33)	225.0(0.5)	40.7(0.1)	16.9(0.1)	11.0
	275.0(0.8)				
1:15	4079(98)	227.0(0.3)	39.3(0.1)	15.6(0.1)	10.0
	263.0(1.1)				

^a Each value is the average of three independent experiments with standard deviation in parentheses. Triplicate measurements were performed for each experiment. ^b The numbers between the two columns for peaks 1 and 2 are the values for the sum of peaks 1 and 2.

galactomannan, implying that the binding site would increase due to the molecular unfolding caused by the superabundant galactomannan. We also calculated dispersed molecular density (M_w/R_g) (39). The conjugates from the 1:3 and 1:6 reactants showed higher density than the others (Table 2). This suggests that the conjugates from the 1:3 and 1:6 reactants consist of more BSA molecules, which are heavier than galactomannan, than those from the 1:9 and 1:15 reactants. A similar trend was also observed with colorimetric measurements.

Conjugates with higher M_w showed a very strong intensity of scattered laser light, even when they existed in extremely small amounts. No tendency was obvious in the formation of higher M_w fractions (over 1 000 000 Da) in every BSA–galactomannan conjugate. Presumably, proteins, polysaccharides, and the conjugates gathered into random aggregates. Hence, the molecules formed were too large to be solubilized or were filtered away during the sample preparation.

Lucey et al. (40), using multiangle laser light scattering, suggested that the R_g values of sodium caseinate with M_w 200 000 and 470 000 Da were 54 and 123 nm, respectively. Thus, R_g (16–17 nm) of the conjugate with $M_w = 250$ 000 Da (Table 2) indicates that the conjugate has a far more compact and globule-like conformation than the elongated sodium caseinate with comparable M_w . Although the molar mass of the conjugate became larger, the R_g of the conjugate was much smaller than that of the sodium caseinate molecule, implying that the conjugate associated compactly. Consequently, the structure of the conjugate might be described as follows: galactomannan is attached to the compact protein surface and encloses it.

Tryptophan shows an emission maximum around 348 nm when dissolved in water (41). It is known that the fluorescence intensity decreases with a red shift of wavelength when protein is denatured and unfolded (42). Kella et al. (29) also reported that native BSA has an emission maximum of 338 nm when excited at 279 nm. In our experiment, little shift of emission maximum wavelength was observed in all conjugates, suggesting that the interior hydrophobic environment of the conjugates was not changed to a great extent (Figure 3). However, the fluorescence intensity of each conjugate was weakened compared with that of the native BSA. Thus, it is thought that the binding of galactomannan occurred at the surface of the BSA molecule and fluorescence from the protein was shielded (12, 43). Among the conjugates, the greatest shielding effect was observed in the 1:15 conjugate with the largest amount of

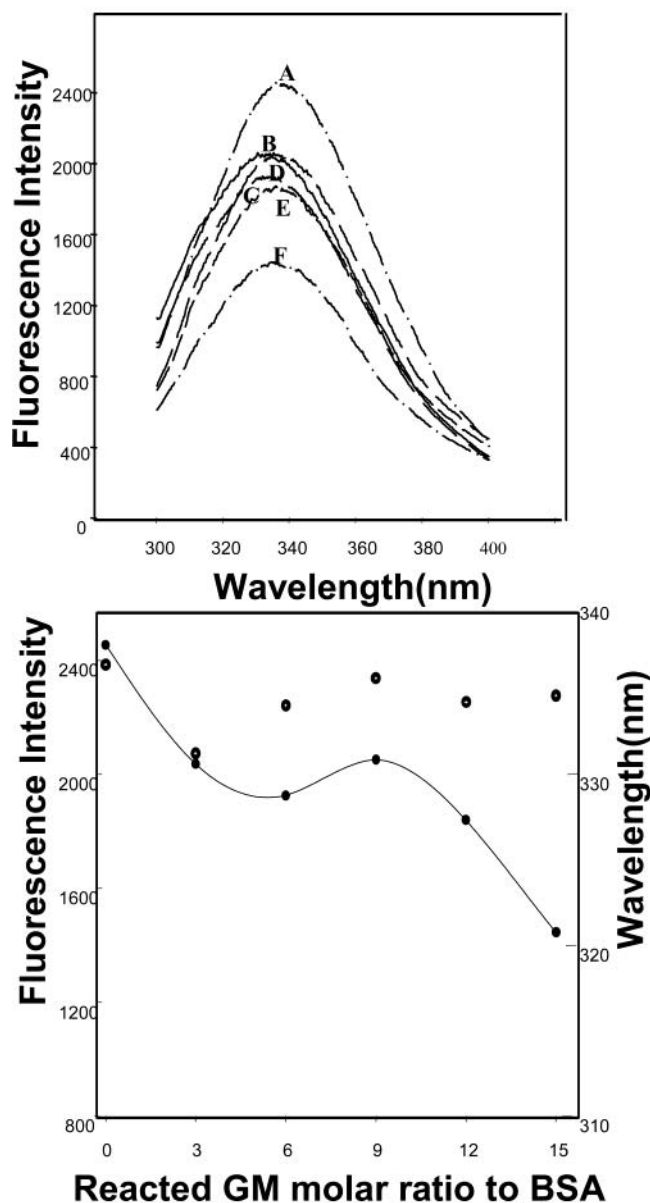


Figure 3. Intrinsic fluorescence spectra of native BSA and BSA–galactomannan conjugates. (A) Native BSA; (B) 1:3 conjugate; (C) 1:6 conjugate; (D) 1:9 conjugate; (E) 1:12 conjugate; (F) 1:15 conjugate. Fluorescence intensity, ●; maximum intensity wavelength, ○.

galactomannan as determined by colorimetry. It could be postulated that the binding of BSA and galactomannan occurred without significant change in the conformation of the BSA molecule.

The extrinsic fluorescence intensity of the conjugates with 1-anilino-8-naphthalenesulfonic acid increased drastically, while the emission maximum remained unchanged (Figure 4). This might be a result of the increase in binding with 1-anilino-8-naphthalenesulfonic acid due to the increment of hydrated hydrophobic surface (45) or the capturing effect of galactomannan, which covers the BSA surface. The surface hydrophobicities of BSA–galactomannan conjugates, calculated on the basis of the initial slope of relative fluorescence intensities of the 1-anilino-8-naphthalenesulfonic acid–protein complex at various concentrations (44), were 689, 554, 550, 620, 581, and 506 for native BSA and the 1:3, 1:6, 1:9, 1:12, and 1:15 reactants, respectively. These results showed that, even though the complex fluorescence intensity itself increased at a certain

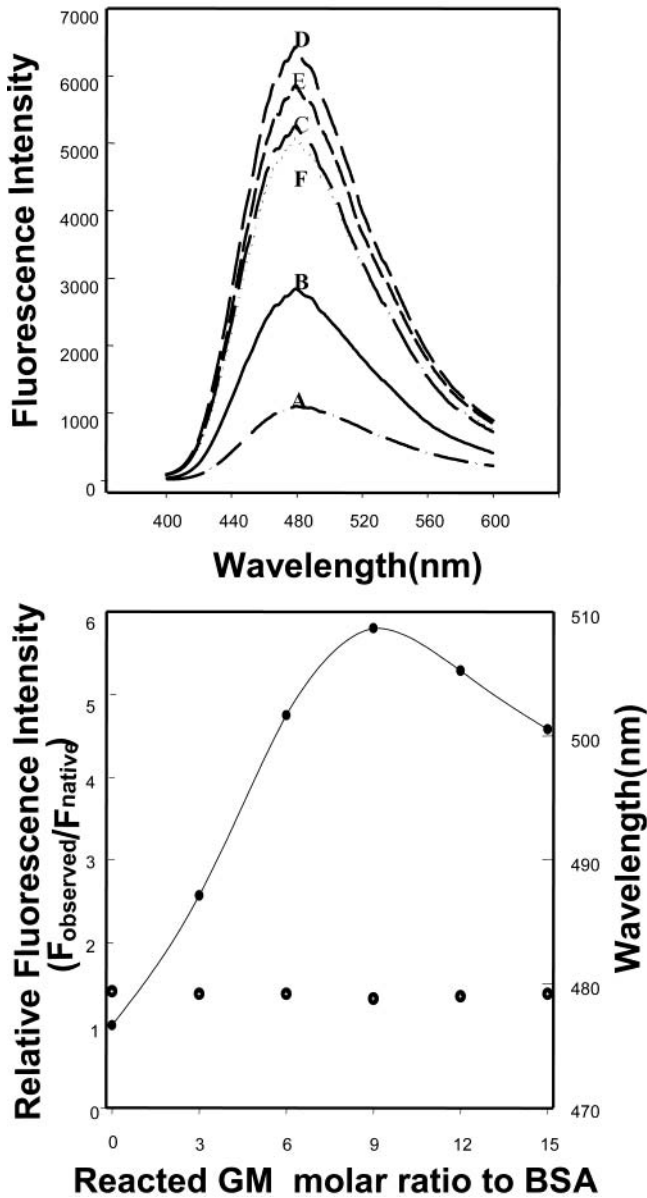


Figure 4. Extrinsic fluorescence spectra of native BSA and BSA–galactomannan conjugates. (A) Native BSA; (B) 1:3 conjugate; (C) 1:6 conjugate; (D) 1:9 conjugate; (E) 1:12 conjugate; (F) 1:15 conjugate. Fluorescence intensity, ●; maximum intensity wavelength, ○.

concentration, the surface hydrophobicity of the conjugate decreased compared with that of the native BSA. Hence, hydrophilic galactomannan is presumed to have covered the BSA surface. It could be concluded that galactomannan complexed with BSA without a significant effect on the BSA peptide backbone.

Native BSA is reported to contain about 55% of the α -helical structure (15). In this experiment, the α -helix content of native BSA was calculated to be 53%, and it remained almost unchanged in all BSA–galactomannan conjugates (Figure 5). Therefore, apparently no change occurred in the secondary structure of BSA upon the formation of the BSA–galactomannan conjugate.

Emulsion Properties of Conjugates. Emulsifying properties were investigated for native BSA and the BSA–galactomannan conjugates with reaction molar ratios of 1:3, 1:6, 1:9, 1:12, and 1:15. The BSA–galactomannan 1:6 conjugate, which had better

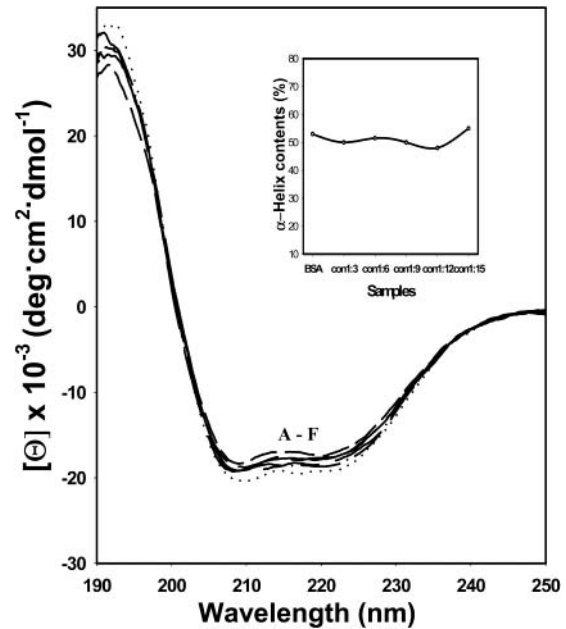


Figure 5. Circular dichroic spectra of various BSA–galactomannan conjugates. (A) Native BSA; (B) 1:3 conjugate; (C) 1:6 conjugate; (D) 1:9 conjugate; (E) 1:12 conjugate; and (F) 1:15 conjugate were analyzed for far-UV circular dichroic spectrum.

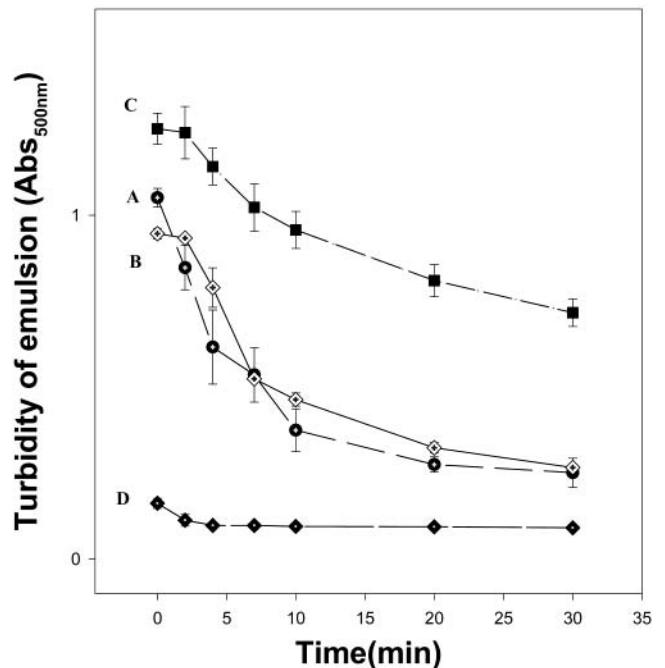


Figure 6. Emulsifying properties of (A) native BSA, (B) native BSA–galactomannan mixture, (C) 1:6 BSA–galactomannan conjugate, and (D) galactomannan. Error bars indicate the standard deviations from three independent experiments.

emulsion stability than the other conjugates, also showed superior emulsifying properties compared to BSA, BSA–galactomannan mixtures, and galactomannan (Figure 6). As the turbidity of the conjugate was higher than that of the mixture, it is suggested that the improvement in the emulsifying properties is due not to the increased continuous phase viscosity from galactomannan, but to the molecular properties of the covalently linked conjugate.

The emulsifying activity index, calculated on the basis of the absorbance, was higher in the conjugate than in the native BSA

Table 3. Various Emulsion Properties of Conjugates

	BSA	conjugate				
		1:3	1:6	1:9	1:12	1:15
emulsifying activity index (m ² /g)	54.4(0.9)	139.5(3.6)	154.3(3.9)	171.4(2.5)	185.4(1.9)	185.7(2.0)
emulsion stability index at pH 7.4	41.7(0.9)	48.0(2.2)	70.5(5.6)	54.5(6.0)	55.7(3.1)	45.5(8.8)
emulsion stability index at pH 2	45.6(3.4)	51.2(2.4)	92.2(2.3)	119.7(2.3)	72.2(1.4)	80.7(3.4)
protein load (mg/m ²)	4.9(0.1)	3.5(0.6)	2.9(0.1)	3.8(0.1)	2.9(0.4)	3.2(0.4)
average emulsion particle size (μm)	1.14(0.03)	1.28(0.22)	1.26(0.03)	1.65(0.03)	1.39(0.18)	1.23(0.17)

^a Each value is the average of three independent experiments with standard deviation in parentheses. Triplicate measurements were performed for each experiment.

(**Table 3**). This indicates that the conjugates adsorbed at a larger droplet area with more unfolded and extended conformation than the native BSA. The membrane thickness, i.e., the amount of protein adsorbed at the oil–water interface measured as protein load (**Table 3**), shows the same results. All conjugates built up a slightly thinner film compared to the native BSA. In general, the more unfolded a molecule, the more it spreads out at the interface (46). We used the same amount of BSA or conjugates (0.1 w/v%) to make emulsions, which means a smaller amount of protein was introduced into the conjugate emulsifier. Hence, the protein in the conjugate unfolds and spreads more at the droplet surface to cover the larger area than the native BSA, following more surface denaturation (47). The emulsion stability index of each conjugate was enhanced compared to that of BSA (**Table 3**) but was not increased in the mere mixture of BSA and galactomannan (**Figure 6**). Thus, the results indicate that the enhancement of the emulsion stability index in the conjugates was caused by the covalently attached galactomannan. Khan et al. (14) suggested that the covalently bonded protein and polysaccharide enhance the emulsifying properties synergistically by reinforcing the adsorption to the oil–water interface and by stabilizing the oil droplets through the viscoelastic layer of polysaccharide in the aqueous phase.

The emulsion stability index of the conjugate also increased when the conjugate formed an emulsion in 1% citric acid solution of pH 2 rather than at neutral pH (**Table 3**). The steric stabilization through covalent attachment of polysaccharide played an important role in the emulsion stability, even under extreme conditions.

The surface activity of the protein depends on the ability of fast adsorption, spreadability, and occupation of a greater area at the interface (48). A highly flexible random-coil protein, compared to a highly ordered compact protein, unfolds more readily and reorients at the interface (49). Hence, it would lead to a faster increase in surface concentration. It would also take greater area per unit protein and show better interfacial activity (48). In our experiment, the average molecular weights of the conjugates increased remarkably compared to the native BSA. The conjugates maintained the secondary structure of native BSA, and the surface hydrophobicity of the conjugates decreased upon the introduction of hydrophilic galactomannan, compared to native BSA. Accordingly, the formation of a conjugate would not render the protein more flexible. Therefore, surface activity would not be increased to lead to faster adsorption at the interface. When small oil droplets are created in a homogenizer, protein adsorbs to the oil–water interface. At an oil–water interface, an adsorbed globular protein is partly in contact with water and partly in contact with oil (2). This change in the molecular environment of the globular protein on adsorption is the major driving force for surface denaturation (50), which increases the surface hydrophobicity of emulsion droplets, resulting in hydrophobic attraction between droplets. Finally, surface denaturation of globular proteins after adsorption to oil

droplet surfaces can lead to extensive flocculation in oil-in-water emulsions (47). At the conjugate-stabilized droplets, protein unfolds more than native BSA, showing a smaller emulsion stability index and protein load. This means that protein-involved hydrophobic interactions between droplets made with the conjugate could be larger than those with protein. However, the emulsion stability was increased in all conjugate emulsifiers. Therefore, it is suggested that the interfacial layer bound to galactomannan physically protects droplets against hydrophobic interactions and subsequent droplet flocculation. The average particle size was in the range of 1–2 μm (**Table 3**). These results suggest that droplet size with the BSA alone or BSA in conjugates was independent of the protein concentration under the conditions used in our experiments.

In conclusion, when the BSA binds with galactomannan to form a conjugate, the ordered structure of native BSA is maintained, and only the conformation of the BSA surface is changed. Structural and conformational analysis suggested that the covalent bond between BSA and galactomannan was formed outward of the α-helical region, and galactomannan contributed to the structural stability of the protein. BSA–galactomannan conjugates adsorbed extensively to the oil phase and maintained an ordered structure at the oil–water interface through covalently bonded galactomannan. The increased emulsifying activity index and emulsion stability index in all conjugates strongly suggested that the improvement in the interfacial properties in conjugates is caused by the physical protection of galactomannan against surface-denatured BSA-involved interdroplet interactions and the viscoelastic interfacial properties due to covalently attached galactomannan.

From a practical point of view, our results suggest that even when BSA is enclosed by galactomannan, it is still capable of undergoing conformation changes at the interface that lead to emulsion instability. However, this can also be prevented by attaching galactomannan. This has important implications for the development of protein-stabilized emulsions, giving a physical barrier to the protein-denaturing conditions, e.g., heating, salts, pH change.

LITERATURE CITED

- (1) Phillips, L. G.; Whitehead, D. M.; Kinsella, J. Functional properties of proteins. In *Structure–Function Properties of Food Proteins*; Phillips, L. G., Whitehead, D. M. Eds.; Academic Press: San Diego, CA, 1994; pp 107–169.
- (2) Damodaran, S. Structure–function relationship of food protein. In *Protein Functionality in Food Systems*; Hettiarachchy, N. S., Ziegler, G. R., Eds.; Marcel Dekker: New York, 1994; pp 1–38.
- (3) Damodaran, S. Interrelationship of molecular and functional properties of food proteins. In *Food Proteins*; Kinsella, J. E., Soucie, W. G., Eds.; The American Oil Chemists' Society: Champaign, IL, 1989; pp 21–51.

- (4) Dickinson, E.; McClements, D. J. Molecular basis of protein functionality. In *Advances in Food Colloids*; Dickinson, E., McClements, D. J. Eds.; Blackie Academic & Professional: London, UK, 1995; pp 27–80.
- (5) Doublier, J. L.; Cuvelier, G. Gums and hydrocolloids: Functional aspects. In *Carbohydrates In Food*; Eliasson, A. C., Ed.; Marcel Dekker: New York, 1996; pp 283–318.
- (6) Dickinson, E.; Euston, S. R. Stability of food emulsions containing both protein and polysaccharide. In *Food Polymers, Gels and Colloids*; Dickinson, E., Ed.; Royal Society of Chemistry: Cambridge, UK, 1991; pp 132–146.
- (7) Babiker, E. E.; Kato, A. Improvement of the functional properties of sorghum protein by protein-polysaccharide and protein–protein complexes. *Nahrung* **1998**, *42*, 286–289.
- (8) Grinberg, V. Y.; Tolstoguzov, V. B. Thermodynamic incompatibility of proteins and polysaccharides in solutions. *Food Hydrocolloids* **1997**, *11*, 145–158.
- (9) Bryant, C. M.; McClements, D. J. Influence of xanthan gum on physical characteristics of heat-denatured whey protein solutions and gels. *Food Hydrocolloids* **2000**, *14*, 383–390.
- (10) Marshall, J. J.; Rabinowitz, M. L. Preparation and characterization of a dextran–trypsin conjugate. *J. Biol. Chem.* **1976**, *251*, 1081–1087.
- (11) Kato, A.; Minaki, K.; Kobayashi, K. Improvement of emulsifying properties of egg white proteins by the attachment of polysaccharide through Maillard reaction in a dry state. *J. Agric. Food Chem.* **1993**, *41*, 540–543.
- (12) Hattori, M.; Imamura, S.; Nagasawa, K.; Takahashi, K. Functional changes of lysozyme by conjugating with carboxymethyl dextran. *Biosci. Biotech. Biochem.* **1994**, *58*, 174–177.
- (13) Kato, A. Preparation and functional properties of protein-polysaccharide conjugates. In *Surface Activity of Proteins*; Magdassi, S., Ed.; Marcel Dekker: New York, 1996; pp 115–130.
- (14) Khan, M. A. S.; Babiker, E. F. E.; Azakami, H.; Kato, A. Molecular mechanism of the excellent emulsifying properties of phosvitin–galactomannan conjugate. *J. Agric. Food Chem.* **1999**, *47*, 2262–2266.
- (15) Peters, T., Jr. Serum albumin. *Adv. Protein Chem.* **1985**, *37*, 161–245.
- (16) Shin, W. S.; Yamashita, H.; Hirose, M. Multiple effects of haemin binding on protease susceptibility of bovine serum albumin and a novel isolation procedure for its large fragment. *J. Biochem.* **1994**, *304*, 81–86.
- (17) Sugio, S.; Kashima, A.; Mochizuki, S.; Noda, M.; Kobayashi, K. Crystal structure of human serum albumin at 2.5 angstrom resolution. *Protein Eng.* **1999**, *12*, 439–446.
- (18) Dea, I. C. M.; Morrison, A. Chemistry and interactions of seed galactomannans. *Adv. Carbohydr. Chem. B* **1975**, *31*, 241–312.
- (19) Fox, J. E. Seed gums. In *Thickening and Gelling Agents for Food*; Imerson, A., Ed.; Blackie Academic & Professional: London, UK, 1992; pp 153–170.
- (20) Robyt, J. F. Polysaccharides I: structure and function. In *Essentials of Carbohydrate Chemistry*; Springer: New York, 1998; pp 172–227.
- (21) Babiker, E. F. E.; Hiroyuki, A.; Matsudomi, N.; Iwata, H.; Ogawa, T.; Bando, N.; Kato, A. Effects of polysaccharide conjugation or transglutaminase treatment on the allergenicity and functional properties of soy protein. *J. Agric. Food Chem.* **1998**, *46*, 866–871.
- (22) Laemmli, U. K. Cleavage of structural proteins during the assembly of the head of bacteriophage T4. *Nature* **1970**, *227*, 680–685.
- (23) Bollag, D. M.; Rozycki, M. D.; Edelstein, S. J. Protein concentration determination. In *Protein Method*; Bollag, D. M., Rozycki, M. D., Edelstein, S. J., Eds; Wiley-Liss, Inc.: New York, 1996; pp 57–81.
- (24) Zacharius, R. M.; Zell, T. E.; Morrison, J. H.; Woodlock, J. J. Glycoprotein staining following electrophoresis on acrylamide gels. *Anal. Biochem.* **1969**, *30*, 148–152.
- (25) Thornton, D. J.; Carlstedt, I.; Sheehan, J. K. Identification of glycoprotein on nitrocellulose membrane and gels. *Methods Mol. Biol.* **1994**, *32*, 119–128.
- (26) Bradford, M. M. A rapid and sensitive method for the quantitation of microgram quantities of protein utilizing the principle of protein–dye binding. *Anal. Biochem.* **1976**, *72*, 248–254.
- (27) Dubois, M.; Gilles, K. A.; Hamilton, J. K.; Rebers, P. A.; Smith, F. Colorimetric method for determination of sugars and related substances. *Anal. Chem.* **1956**, *28*, 350–356.
- (28) Wyatt, P. J. Light scattering and the absolute characterization of macromolecules. *Anal. Chim. Acta.* **1993**, *272*, 1–40.
- (29) Kella, N. K. D.; Kang, Y. J.; Kinsella, J. E. Effect of oxidative sulfitolysis of disulfide bonds of bovine serum albumin on its structural properties: A physicochemical study. *J. Protein Chem.* **1988**, *7*, 535–548.
- (30) Chen, Y. H.; Yang, J. T.; Martinez, H. M. Determination of the secondary structures of proteins by circular dichroism and optical rotatory dispersion. *Biochemistry* **1972**, *11*, 4120–4133.
- (31) Pearce, K. N.; Kinsella, J. E. Emulsifying properties of proteins: Evaluation of a turbidimetric technique. *J. Agric. Food Chem.* **1978**, *26*, 716–723.
- (32) Liu, M.; Damodaran, S. Effects of transglutaminase-catalyzed polymerization of β -casein on its emulsifying properties. *J. Agric. Food Chem.* **1999**, *47*, 1514–1519.
- (33) Qi, M.; Hettiarachchy, N. S.; Kalapathy, U. Solubility and emulsifying properties of soy protein isolates modified by pancreatin. *J. Food Sci.* **1997**, *62*, 1110–1115.
- (34) Dickinson, E. Emulsion stability. In *Advances in Food Emulsions and Foams*; Dickinson, E., Stainsby, G., Eds.; Elsevier Applied Science: London, UK, 1988; pp 1–44.
- (35) Shu, Y. U.; Sahara, S.; Nakamura, S.; Kato, A. Effects of the length of polysaccharide chains on the functional properties of the Maillard-type lysozyme-polysaccharide conjugate. *J. Agric. Food Chem.* **1996**, *44*, 2544–2548.
- (36) Nakamura, S.; Kobayashi, K.; Kato, A. Role of positive charge of lysozyme in the excellent emulsifying properties of Maillard type lysozyme–polysaccharide conjugate. *J. Agric. Food Chem.* **1994**, *42*, 2688–2691.
- (37) Matsudomi, N.; Inoue, Y.; Nakashima, H.; Kato, A.; Kibayashi, K. Emulsion stabilization by Maillard-type covalent complex of plasma protein with galactomannan. *J. Food Sci.* **1995**, *60*, 265–268.
- (38) Van Holde, K. E. Solutions of macromolecules. In *Physical Biochemistry*, 2nd ed.; Van Holde, K. E., Ed.; Prentice-Hall: Englewood Cliffs, NJ, 1985; pp 24–50.
- (39) Yoo, S. H.; Jane, J. L. Molecular weights and gyration radii of amylopectins determined by high-performance size-exclusion chromatography equipped with multi-angle laser-light scattering and refractive index detectors. *Carbohydr. Polym.* **2002**, *49*, 307–314.
- (40) Lucey, J. A.; Srinivasan, M.; Singh, H.; Munro, P. A. Characterization of commercial and experimental sodium caseinates by multiangle laser light scattering and size-exclusion chromatography. *J. Agric. Food Chem.* **2000**, *48*, 1610–1616.
- (41) Ma, C.-Y.; Harwalkar, V. R. Study of thermal denaturation of oat globulin by ultraviolet and fluorescence spectrophotometry. *J. Agric. Food Chem.* **1988**, *36*, 155–160.
- (42) Lakkis, J.; Villota, R. Effect of acylation on substructural properties of proteins: A study using fluorescence and circular dichroism. *J. Agric. Food Chem.* **1992**, *40*, 553–960.
- (43) Hattori, M.; Numamoto, K.; Kobayashi, K.; Takahashi, K. Functional changes in β -lactoglobulin by conjugation with cationic saccharides. *J. Agric. Food Chem.* **2000**, *48*, 2050–2056.
- (44) Kato, A.; Nakai, S. Hydrophobicity determined by a fluorescence probe method and its correlation with surface properties of proteins. *Biochim. Biophys. Acta* **1980**, *624*, 13–20.
- (45) Guha, S.; Bhattacharyya, B. A partially folded intermediate during tubulin unfolding: Its detection and spectroscopic characterization. *Biochemistry* **1995**, *34*, 6925–6931.

- (46) Evans, M. T. A.; Phillips, M. C.; Jones, M. N. The conformation and aggregation of bovine β -casein A. *Biopolymers* **1979**, *18*, 1123–1127.
- (47) Kim, H. J.; Decker, E. A.; McClements, D. J. Role of postadsorption conformation changes of β -lactoglobulin on its ability to stabilize oil droplets against flocculation during heating at neutral pH. *Langmuir* **2002**, *18*, 7577–7583.
- (48) Hill, S. E. Emulsions. In *Methods of testing protein functionality*; Hall, G. M., Ed.; Blackie Academic & Professional: New York, 1996; pp 153–185.
- (49) Song, K. B.; Damodaran, S. Structure–function relationship of proteins: adsorption of structural intermediates of bovine serum albumin at the air–water interface. *J. Agric. Food Chem.* **1987**, *35*, 236–241.
- (50) MacRitchie, F. Reversibility of protein adsorption. In *Proteins at Liquid Interfaces*; Möbius, D., Miller, R., Eds.; Elsevier Science: London, UK, 1998; pp 149–177.

Received for review June 21, 2002. Revised manuscript received November 7, 2002. Accepted November 10, 2002. This research was supported by a grant from the National Research Lab. Program, funded by the Ministry of Science and Technology of Republic of Korea. S.J.C. acknowledges a graduate fellowship provided by the Ministry of Education through the Brain Korea 21 Project.

JF020698V